ELSEVIER

Applied Surface Science 175–176 (2001) 195–200

applied surface science

www.elsevier.nl/locate/apsusc

# Correlated surface bands of the prototypical interface Sn/Si(1 1 1)-α-$\sqrt{3}$

A. Charrier[a,*], R. Pérez[b], F. Thibaudau[a], J.-M. Debever[a], J. Ortega[b], F. Flores[b], J.-M. Themlin[a]

[a]*Groupe de Physique des Etats Condensés, UMR CNRS 6631, Faculté des Sciences de Luminy, Université de la Méditerranée, Case 901, 13288 Marseille Cedex 9, France*

[b]*Departemento de Física Teórica de la Materia Condensada, Facultad de Ciencias, Universidad Autónoma de Madrid, Madrid 28049, Spain*

Accepted 30 July 2000

**Abstract**

Using angle-resolved inverse photoemission spectroscopy (KRIPES), we have investigated the unoccupied electronic structure of the model interface Sn/Si(1 1 1)-α-$\sqrt{3}$ at room temperature. In addition to a ''metallic'' surface state crossing the Fermi level ($E_F$) near the $\overline{K'}$ point, we unambiguously assign a second feature of our KRIPES spectra, located around 1.5 eV above $E_F$, to a second surface state $U_2'$. We will experimentally show that $U_2'$ is an intrinsic feature of the α-$\sqrt{3}$ reconstruction which cannot be associated with defects. The existence of these two surface states is not compatible with the ideal $T_4$ model which would show either a single, half-occupied metallic band crossing $E_F$, or an insulating phase if strong correlation effects, important for these narrow surface bands, are considered. Rather, both $U_1'$ and $U_2'$ receive a natural explanation, once many-body effects are introduced, in the framework of a dynamical fluctuations model, where two kinds of Sn adatoms sites reminiscent of a low-temperature $3 \times 3$ phase do persist at room temperature. Correlated surface bands incorporating many-body effects in a non restricted way provide a complete description of the experimental surface bands and their dispersions.


*Keywords:* Inverse photoemission; Electronic structure; Many-body effects

## 1. Introduction

The α-($\sqrt{3} \times \sqrt{3}$)$R30^\circ$ reconstruction (hereafter called $\sqrt{3}$ for brevity) is induced by the adsorption of 1/3 ML of trivalent and tetravalent adatoms on Si(1 1 1) and Ge(1 1 1) [1,2]. This surface which is an old and familiar object in surface science, is believed to be described by an adatom $T_4$ model which involves the presence of a single type of adatom site. In this model, adatoms are located directly above a second layer substrate atom and bind to three atoms in the substrate first layer [3]. For tetravalent adatoms, three electrons are involved in the covalent bonding with the substrate and one electron fills the dangling bond, and we expect a metallic character for this surface. Using $k_{//}$-resolved inverse photoemission spectroscopy (KRIPES), we show that it is essential to take into account correlation effects to describe these (supposedly) half-filled and narrow surface bands. In the limit of strong correlation effects, like in the case of

* Corresponding author.
*E-mail address*: charrier@gpec.univ-mrs.fr (A. Charrier).

0169-4332/01/$ – see front matter 
PII: S0169-4332(01)00061-7

$\sqrt{3}$-SiC(0 0 0 1), a Mott–Hubbard transition may occur, with a gap opening, and the surface is semiconducting [4].

We will show that the α-$\sqrt{3}$-Sn/Si(1 1 1) do present a metallic state. This state, mainly unoccupied, can be followed in a large portion of the SBZ and crosses the Fermi level around $\overline{K}'$. The overall bandwidth of this state being around 0.55 eV, correlation effects are expected to play some role. Moreover, in addition to this state, our results indicate the presence of a second empty surface state localized 1.5 eV above $E_F$. The presence of this state is hardly compatible with a single $T_4$ site but rather suggests that more than one site is involved in the α-$\sqrt{3}$ reconstruction. The same conclusion has been reached following photoemission measurements where two components were found in the Sn 4d core level [5]. Similar results have been obtained for Pb(Sn)/Ge(1 1 1) [6,7] for which a reversible phase transition α-$\sqrt{3}$ (room temperature: RT) $\leftrightarrow 3 \times 3$ (low temperature: LT) [2] has been discovered. Using first-principles computer simulations, this transition has been interpreted in terms of order/disorder phase transition where the adatoms fluctuate between two positions at RT and stabilized in a $3 \times 3$ at low temperature [7].

Substitutional Si adatom is the dominant defect, and its concentration can be varied in an extended range in a two-dimensional solid solution $Sn_{1-x}Si_x$/Si(1 1 1) with $x \leq 0.5$. In addition to the α-phase ($x \approx 0.03$), we have also investigated the other limiting case $x = 0.5$, known as the γ- or mosaic phase, as well as an intermediate phase around $x \approx 0.4$. KRIPES spectra on these highly defective surfaces reveal characteristic signatures on the empty states. They do confirm that the two states $U_1'$ and $U_2'$ detected on the α-$\sqrt{3}$ are intrinsic to the ideal $\sqrt{3}$ reconstruction and cannot be attributed to defects. These two surface bands $U_1'$ and $U_2'$ receive natural explanation, once correlation effects are appropriately taken into account [12], in the framework of this dynamical fluctuations model as originating from a dynamic $3 \times 3$ periodicity.

On the other hand, recent X-ray diffraction data of Sn/Ge(1 1 1) do not support this interpretation [8,9], suggesting rather a unique $T_4$ site for Sn adatoms in the $\sqrt{3}$ reconstruction observed at RT. Other authors have stressed out the crucial role played by defects in the $3 \times 3 \leftrightarrow \sqrt{3}$ phase transition [9,10]. It has been shown that a remnant of the LT $3 \times 3$ phase could be stabilized at RT around substitutionals Ge adatoms on a significant fraction of the surface [9], in coexistence with an unperturbed α-$\sqrt{3}$ phase. These defects may thus severely complicate the interpretation of existing results. However, it has been shown that for the isoelectronic system Sn/Si(1 1 1)-α-$\sqrt{3}$, the defect-induced $3 \times 3$ perturbations at RT have a much shorter extension in comparison to Sn/Ge(1 1 1) [11]; it is thus a better testing ground to tackle the validity of the adatom $T_4$ model.

## 2. Experimental procedures

The experiments have been performed in an ultra-high-vacuum chamber (base pressure $3 \times 10^{-10}$ mbar) equipped with a low-energy electron diffractometer (LEED) and the inverse photoemission set-up [13]. The latter consists of an electron gun and an elliptical mirror to focus photons emitted in a large solid angle towards the photon detector. The Geiger-müller type detector filled with a helium–iodine mixture and sealed with a $SrF_2$ window operates in an isochromat mode at a fixed photon energy of 9.5 eV. The overall energy resolution, determined by measuring the Fermi edge on a Ta foil, is 0.35 eV, including the electron gun and the detector. The dispersion within the surface Brillouin zone (SBZ) of interest is investigated by rotating the electron gun in a vertical plane perpendicular to the sample surface (variable polar angles with respect to the surface normal) and oriented along a given azimuth.

We have used phosphorus-doped (resistivity $\sim 2 \times 10^{-2}$ Ω cm) Si(1 1 1) wafertype samples of size 15 mm × 5 mm × 0.28 mm. Before introducing into vacuum, the sample is chemically prepared ex situ by a wet hydrogenation procedure. The sample is then annealed under UHV by electron bombardment on its backside using a BaO cathode. Annealing temperature was monitored by an infrared pyrometer assuming an emissivity of 0.8. The starting point before Sn evaporation was the $7 \times 7$ reconstruction obtained by short annealing around 1100°C. In order to obtain the α-$\sqrt{3}$ phase, we have deposited approximately 1.5 ML of Sn at room temperature followed by annealing at 630°C for 4 min. The quality of all surface reconstructions and their orientation was checked out by LEED. The details of this procedure were also

checked in a separate set-up using STM, which in contrast to LEED allows an easy determination of the defect concentration $x$.

## 3. Experimental results

Fig. 1 shows KRIPES spectra obtained along the two high symmetry directions $\overline{\Gamma K'}$ and $\overline{\Gamma M'}$ of the reconstructed SBZ. These spectra give the number of detected photons normalized by the incident current flowing through the sample versus the electron energy, with respect to $E_F$. The position of the different empty states is obtained by removing a background line to the raw data and then fitting each spectrum by a set of gaussians. The maximum of each gaussian which indicates the presence of an empty state is marked by a vertical bar.

These spectra show the presence of five different empty states located in the range 0–5 eV above $E_F$. The origin of these states has been identified by saturating the dangling bonds without modifying the surface reconstruction. Fig. 2(1) shows how the two states closest to $E_F$, $U'_1$ and $U'_2$ (a), are attenuated after exposure of about 1 l of activated hydrogen (b); they

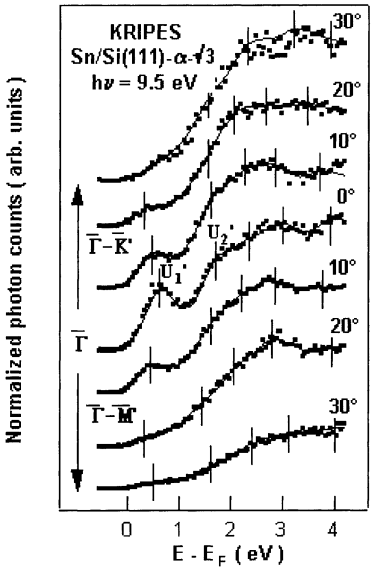


Fig. 1. KRIPES spectra obtained on the α-$\sqrt{3}$ phase along the $\overline{\Gamma K'}$ and $\overline{\Gamma M'}$ directions of the surface Brillouin zone. Each vertical bar marks the presence of an empty state.

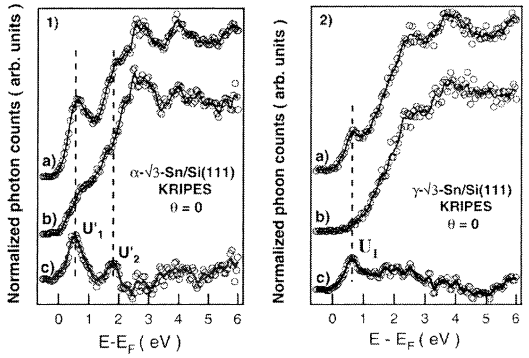


Fig. 2. KRIPES spectra of: (1) α- and (2) γ-phases. (a) Initials spectra; (b) after hydrogenation; (c) difference between the two previous ones.

are thus attributed to surface states. This attenuation is emphasized on part (c), which is the difference between the two previous spectra. The upper states which remain almost unchanged are thus rather attributed to bulk states. In the following, we will mainly focus on the surface states, $U'_1$ and $U'_2$, respectively, located around 0.45 and 1.6 eV above $E_F$.

For both states, and in both directions $\overline{\Gamma K'}$ and $\overline{\Gamma M'}$, the intensity is maximum at normal incidence (SBZ center) and decreases as the angle of incidence of the electrons increases (SBZ edges). In the $\overline{\Gamma M'}$ directions, $U'_1$ and $U'_2$ can be followed along this azimuth for every angle and therefore do not cross $E_F$. However, along the $\overline{\Gamma K'}$ direction both peaks tend to get closer to $E_F$ as the angle increases and $U'_1$ finally vanishes around 27°, which indicates a clear Fermi level crossing. While $U'_1$ and the metallic character of this surface can be explained by a simple adatom $T_4$ model, provided correlation effects are small or negligible, the existence of this second state, $U'_2$, is incompatible with this model.

Some authors [9,10] have recently stressed out the crucial role played by defects, which could possibly influence photoemission spectra. Fig. 3 shows KRIPES spectra obtained on (a) the α-$\sqrt{3}$ phase; (b) an intermediate phase containing about 0.25 ML of Sn (25% of substitutional Si adatoms) and (c) on the mosaic phase containing 50% substitutional Si adatom defects. It is clear from Fig. 3 that the intensity of $U'_2$ is larger on α-$\sqrt{3}$. Furthermore, although small shoulders around 1.6 eV can be distinguished in the non-ideal cases, activated hydrogen spectra taken after

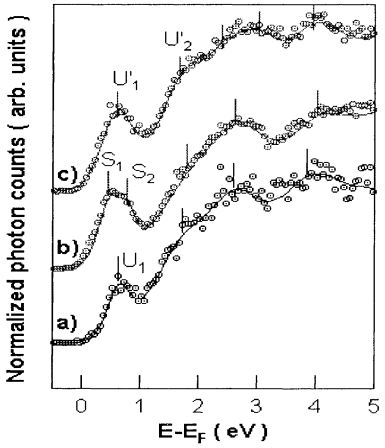


Fig. 3. KRIPES spectra of (a) the γ-phase; (b) an intermediate phase and (c) the α-phase. Labeled peaks or shoulders are attributed to surface states.

exposure (see Fig. 2b for the γ-phase) do show that these shoulders cannot be attributed to surface states [14]. These results let us conclude that $U_2'$ cannot be attributed to substitutional Si adatoms, but is really intrinsic to the ideal α-$\sqrt{3}$ reconstruction. Another structural model than the $T_4$ one must thus be considered to explain this second empty surface state.

Fig. 4 shows the band dispersion for these two surface states. We notice that they disperse the same way although they do not have the same bandwidth, $U_1'$ ($W_1' = 0.55$ eV) being larger than $U_2'$ ($W_2' = 0.4$ eV). The rather small bandwidths measured for

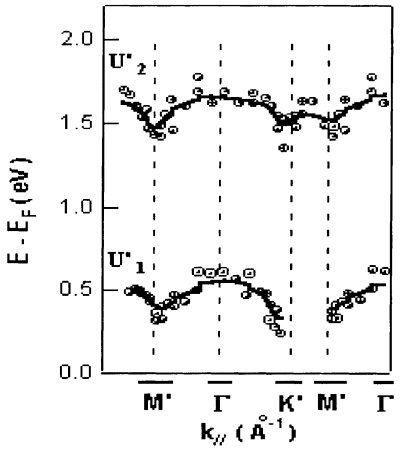


Fig. 4. Band dispersion of the α-phase.

these bands suggest that correlation effects may play an important role on this reconstruction.

For Sn/Ge(1 1 1), the reversible phase transition α-$\sqrt{3} \leftrightarrow 3 \times 3$ has been studied by photoemission [7]. These authors found both below and above the transition two components in the Sn 4d core level as well as a band splitting in the valence band giving rise to two surface states, one crossing the Fermi level, and the other one below it. Theoretical calculations [7] have shown that these states may be due to two kinds of Sn adatoms that fluctuate between two positions at RT and stabilize in a $3 \times 3$ at LT.

These adatom positions which correspond to the positions of the adatoms in the $3 \times 3$ [15] are still on the $T_4$ site with two different lengths above the Si terminating layer. The $3 \times 3$ unit cell contains three adatoms; each brings one unpaired electron. One of these adatoms is higher than the other two with respect to the Si compact plane. A charge transfer which occurs from a lower adatom to the higher adatom gives rise to two surface states, one empty and one occupied observed in ARUPS. The second lower adatom remains half-occupied and gives rise to a metallic state. The different occupied surface states observed on this interface have thus been explained on the basis of this dynamical reconstruction.

For Sn/Si(1 1 1) the same kind of results has been found, with two components in the Sn 4d core level. Although a complete phase transition has not been observed yet for this interface we can reasonably expect the same kind of process [11,16]. In order to verify our hypothesis, we have realized electronic structure calculations including many-body effects.

## 4. DFT-LDA and many-body calculations

Starting from a $3 \times 3$ unit cell, the surface geometry has been optimized by minimizing the total energy by means of a local orbital, self-consistent LDA-DFT method [17]. The relaxed surface is a $3 \times 3$ unit cell where one adatom is displaced upwards and the other two adatoms displaced downwards with respect to the ideal position of the adatoms in the usual $\sqrt{3}$ geometry, with a total distortion of 0.3 Å.

Fig. 5 shows the bands resulting from the calculations. Of the three LDA bands, represented by dotted lines, one is located at about 0.1 eV under $E_F$ and is

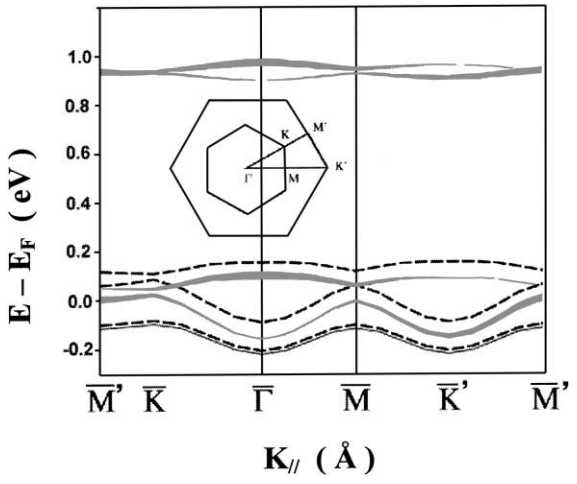


Fig. 5. Theoretical DFT-LDA bands (dashed lines) and correlated bands (continuous lines) from many-body calculations.

fully occupied, with a weight of two electrons. This state is mainly localized on the upper adatom. The two upper bands, which can accommodate four electrons, are actually filled by a single one and are both mainly localized on the two lowest equivalent adatoms. Thus, it appears that a charge transfer occurs from one of the lower adatoms towards the upper one, giving rise to an occupied state mainly localized on the upper adatom and an empty state mainly localized on this lower adatom. The second lower adatom stays half filled and gives rise to a state that crosses the Fermi level.

These bands present a relatively small bandwidth, $W \leq 0.35$ eV, and correlation effects on the surface are thus thought to be important [2,18]. The effective intra-site Coulomb interaction $U_{\text{eff}} = 1.15$ eV, has been estimated by restricted LDA calculations where the filling factors of the surface were varied and the effect of these changes on the surface band levels evaluated [12]. In order to describe the experimental data, many-body effects have thus to be taken into account with the introduction of a Hubbard Hamiltonian [12] in our $3 \times 3$ model. The full lines represented on Fig. 5 show the correlated bands obtained through the Hubbard Hamiltonian. Unlike the occupied bands which were practically unchanged, the two upper bands have been split in two groups of two correlated bands. The first group crosses $E_F$; its bands are parallel to the two upper LDA bands and their bandwidth is not changed. These bands mainly appear in the empty states and are thus ascribed to $U'_1$. The other two correlated bands of the upper group are localized 1 eV above $E_F$ and have a total weight of one electron. These bands, which have a reduced bandwidth, explain the presence of $U'_2$ observed in KRIPES.

We still have to explain how the dispersion of the theoretical surface bands calculated in the $3 \times 3$ SBZ reproduces the dispersion of the experimental surface bands measured on the $\sqrt{3} \times \sqrt{3}$ SBZ. In order to evaluate the matrix elements involved in direct and inverse photoemission along the various symmetry lines of the $3 \times 3$ SBZ, we have optimized a simple tight-binding model with the LDA surface bands near $E_F$. In Fig. 5, the thickness of the solid line representing the correlated bands corresponds to the strength of the matrix elements correlated in an extended zone scheme. It is clear that the portions of the $3 \times 3$ bands with high matrix elements broadly reproduce the observed dispersion of $U'_1$ and $U'_2$ in the $\sqrt{3} \times \sqrt{3}$ SBZ.

## 5. Conclusions

Finally, we have revealed on the prototypical, ideal Sn/Si(1 1 1)-$\sqrt{3}$-$\alpha$ reconstruction the presence of two surface states: $U'_1$ which crosses $E_F$, and $U'_2$, located about 1.5 eV above it. The presence of a additional surface state, $U'_2$, cannot be explained with the unique $T_4$ site of the ideal $T_4$ model. The structure of this surface is well understood in term of a dynamical fluctuations model, once many-body effects are properly taken into account. We have experimentally shown that $U'_2$ cannot be attributed to defects. Rather, it is an intrinsic feature of the $\alpha$-$\sqrt{3}$ reconstruction.

## References

[1] C.A. Sebenne, in: Fu-Jia Yang, et al. (Eds.), Surface Physics and Related Topics, World Scientific, Singapore, 1991, p. 259.
[2] J.M. Carpinelli, H.H. Weitering, M. Bartkowiak, R. Stumpf, E.W. Plummer, Phys. Rev. Lett. 79 (1997) 2859.
[3] J.E. Northrup, J. Neugebauer, Phys. Rev. B 52 (1995) R17001.
[4] J.-M. Themlin, I. Forbeaux, V. Langlais, H. Belkhir, J.-M. Debever, Europhys. Lett. 39 (1997) 61.
[5] M. Göthelid, M. Björkqvist, T.M. Grehk, G. Le Lay, U.O. Karlsson, Phys. Rev. B 52 (1995) R14352.

[6] R.I.G. Uhrberg, T. Balasubramanian, Phys. Rev. Lett. 81 (1998) 2108.
[7] J. Avila, A. Mascaraque, E.G. Michel, M.-C. Asensio, G. Le Lay, J. Ortega, R. Pérez, F. Florés, Phys. Rev. Lett. 82 (1999) 442.
[8] P. Bunk, J.H. Zeysig, G. Falkenberg, R.L. Johnson, M. Nelsen, M.M. Nielsen, R. Feidenhans'l, Phys. Rev. Lett. 83 (1996) 2226.
[9] A.V. Melechko, J. Braun, H.H. Weitering, E.W. Plummer, Phys. Rev. B 61 (2000) 2235.
[10] T.E. Kidd, T. Miller, T.-C. Chiang, Phys. Rev. Lett. 83 (1999) 2789.
[11] L. Ottaviano, M. Crivellari, L. Lozzi, S. Santucci, Surf. Sci. 445 (2000) L41.
[12] F. Flores, J. Ortega, R. Pérez, Surf. Rev. Lett. 6 (1999) 411.
[13] S. Bouzidi, F. Coletti, J.-M. Debever, P.A. Thiry, P. Dumas, Y. Chabal, Phys. Rev. B 45 (1992) 1187.
[14] A. Charrier, F. Thibaudau, J.-M. Debever, J.-M. Themlin, submitted for publication.
[15] J. Avila, Y. Huttel, A. Mascaraque, G. Le Lay, E.G. Michel, M.C. Asensio, Surf. Sci. 433–435 (1999) 327.
[16] J. Slezák, P. Mutombo, V. Cháb, Phys. Rev. B 60 (1999) 13328.
[17] A.A. Demkov, J. Ortega, O.F. Sankey, M.P. Grumbach, Phys. Rev. B 52 (1995) 1618.
[18] A. Goldoni, S. Modesti, Phys. Rev. Lett. 79 (1997) 3266.